Hindawi Publishing Corporation
International Journal of Antennas and Propagation
Volume 2014, Article ID 403871, 10 pages
http://dx.doi.org/10.1155/2014/403871

Research Article

Multishorting Pins PIFA Design for Multiband Communications

Muhammad Sajjad Ahmad, C. Y. Kim, and J. G. Park

School of Electronics Engineering, Kyungpook National University, 1370 Sankyuk-Dong, Buk-Gu, Daegu 702-701, Republic of Korea

Correspondence should be addressed to C. Y. Kim; cykim@ee.knu.ac.kr

Received 6 October 2013; Revised 16 December 2013; Accepted 17 December 2013; Published 5 February 2014

Academic Editor: Bing Liu

A novel PIFA model with multiple shorting pins is proposed for multiband, low profile wireless applications, which has the ability to work in adverse conditions. The proposed model has a planar radiating sheet, a ground plane, and sides covered with PEC boundaries. The substrate inside the *antenna box* is tempered in order to improve the bandwidth and gain. The enhancements applied to the proposed PIFA model show improved characteristics for this PIFA model and make it a versatile candidate for handheld, low profile, and multiband resonant communication devices. Pertinent communication devices are those that work with GSM 850/900, UMTS 850/900/1700/1900/2100, LTE 2300/2500, and ISM 2400 bands used for Bluetooth and WLAN.

1. Introduction

Antennas (electromagnetic waves guiding devices) radiate signals to unbounded mediums. They are frequency dependent devices and are designed to operate at specific frequencies known as the antenna's operating bands. Other than these specific frequency bands, an antenna rejects any signal that is fed to it. Antennas are known for their various properties including gain, directivity, radiation pattern, specific absorption rate (SAR), and Voltage Standing Wave Ratio (VSWR).

In [1–3] modified planar inverted-F antenna (PIFA) models were proposed with compact size, multiple resonant bands, and enhanced bandwidth by changing the width of the shorting and feed pins, adding a parasitic element parallel to the shorting pin at an optimized distance and a planar rectangular monopole top loaded with two rectangular patches with one of them grounded, respectively. In an ordinary PIFA model, when a shorting pin is applied near the feeding point, it allows the design to be reduced in size but narrows the bandwidth at the same time. By applying different schemes and techniques to an ordinary PIFA model, we can enhance not only its bandwidth but also its gain and efficiency as well.

In recent years, the antenna industry has shown a rapid demand for multiband resonant, low profile, and ultrawide bandwidth antennas [4]. The fact that PIFA has a flexible design and can provide multiband resonant operations makes it a favorable candidate for the antenna industry. Introducing slots in the radiating patch may allow designers to achieve resonant frequencies that are not possible for a conventional PIFA with small dimensions to resonate on. Moreover, with slots in the ground plane of a PIFA model, it is reported in the literature as a bandwidth enhancement method [5]. Such PIFA models, commonly known as a meandered ground plane or meandered radiating patch, have diversified PIFAs for the low profile design industry. Plenty of modified PIFA models have been designed for multiband operations; slotted PIFA, meandered ground plane PIFA, and multiple shorting pins PIFA have been successful among others. In [6, 7], the limitations of electrically small antennas in terms of the gain, bandwidth, and their capacity to produce the desired number of resonant bands along with guidelines to design such antennas based on the parametric analysis of electrically small antennas are discussed.

Antennas are designed and tested in almost ideal environments, but when they are exposed to conducting materials in their surroundings, they do not just shift their resonant frequency but the bandwidth and gain are changed as well. The performance of any conventional antenna is affected severely, in terms of its resonant frequency, gain,

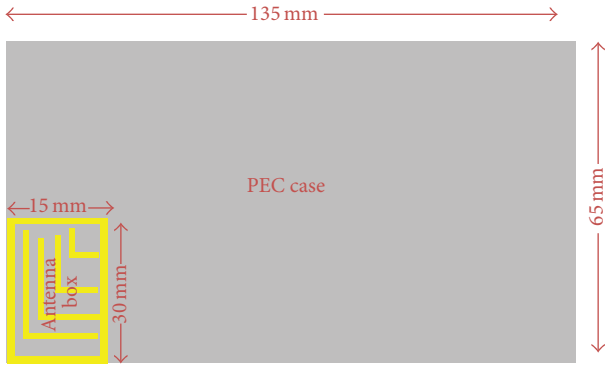

Figure 1: Proposed PIFA model *antenna box* and *PEC case*, with PEC boundaries around it.

and bandwidth, in the presence of conducting bodies around the antenna. It is considered a loophole for communication devices working with such antennas. In [8, 9], the impact of metallic surfaces and user's hand on the performance of different antennas are discussed. The efficiency of the antenna is reported to drop from 91% (without the hand's effect) to 41% (with the hand's effect), which might not be acceptable for communication devices which require higher efficiency. Therefore, an exquisite antenna design is needed for today's industry which can cope with such undesired situations and maintain its efficiency even in the worst conditions. Our proposed model has the ability to maintain its performance in such critical conditions. Details of our proposed antenna design are given in the following section.

2. Antenna Design Procedure

The proposed antenna model is shown in Figure 1. It consists of a dielectric material FR-4, which has a dielectric constant of $\varepsilon_r = 4.4$ and a thickness of 7 mm, *antenna box*, and *PEC case*. The dielectric material is sandwiched between the radiating patch (top sheet of the *antenna box*) and the ground plane of the *PEC case*. The dimensions of the proposed model are $65 \times 135 \times 7\ \text{mm}^3$. For simplicity the model is divided in two main sections: firstly, the *PEC case* and second the *antenna box*. The dimensions of the *antenna box* are $30 \times 15 \times 7\ \text{mm}^3$. The top sheet of *antenna box* acts as a radiating patch which contains slots around its boundary to maintain the separation between the antenna elements and the *PEC case*. In Figures 2 and 3, a 3D view of the proposed model is shown with special emphasis on the *antenna box* and its components, that is, the radiating patch, parasitic patch, feeding position, and shorting pins. A parametric description for the radiation patch is presented in Figure 4, with detail of the parameters in Table 1. Slots in the radiating patch are used to increase the electrical length of the radiating patch in order to achieve the resonant band at lower frequencies. The sides of the *antenna box* are acting as parasitic patch elements. A prototype of the proposed model is designed and shown in Figure 8.

The proposed model contains three shorting pins, shown in Figure 3, that are connecting the radiating patch to the ground plane at different point. The width of each shorting pin is 1 mm and the height is 7 mm. Thickness of the model is 7 mm. The width of the lumped port feeding sheet is 2 mm and the direction of integration line for the modes excitation is along the z-axis. The distance between consecutive shorting pins can be changed to shift the resonant bands if desired. Multiple shorting pins and a shortening pin are used to add stability to this model and to obtain multiple resonant bands [10, 11]. Because the boundaries are PEC and the PIFA antenna models are known for their narrow band operations, we used the two sides of the *antenna box* as a parasitic patch. In [12, 13], the parasitic patch for microstrip antennas was introduced and a bandwidth enhancement of 25.5% was reported. It was established that multiple parasitic patches can be used for bandwidth enhancement purposes, both in the vertical and horizontal positions. In our model, the parasitic patch is perpendicular to the driving patch and is connected to the ground plane through the shortening pin.

Table 1: Length of the slots inserted in the radiating patch.

Slot name	Length (mm)
L_A	30
L_B	30
W_A	15
W_B	15
L_1	6.5
L_2	15
L_3	18
L_4	25
L_5	13
L_6	5
L_7	8
L_8	10

2.1. Slots in the Radiating Patch. Slots are inserted in the radiating patch to increase the electrical length of the radiating patch. The width of the slots in the radiating patch is 0.5 mm and is denoted by s; the slot lengths were different and are given in Table 1. The slots around the boundary of radiating patch, that is, L_A, L_B, W_A, and W_B, are used to maintain a separation between the antenna elements of the *antenna box* and *PEC case*; their width is fixed to 1 mm. Although the width and length of the slots help us to change the resonant frequency bands, the interslot coupling effect cannot be neglected either. Both the distance between the slots and their width allow us to tune our model to a suitable coupling effect for desired S11 results.

It is known that the small size of a radiating patch has a limit for producing resonant bands at lower frequencies; a well-tuned slotted model can achieve resonant bands at lower frequencies and may improve the performance of the model [14]. Using the fact that inserting a slot in the radiating patch may result in a new resonant frequency, the position and length of the slot to be inserted in the radiating patch for a desired resonant frequency can be approximately predicted [15].

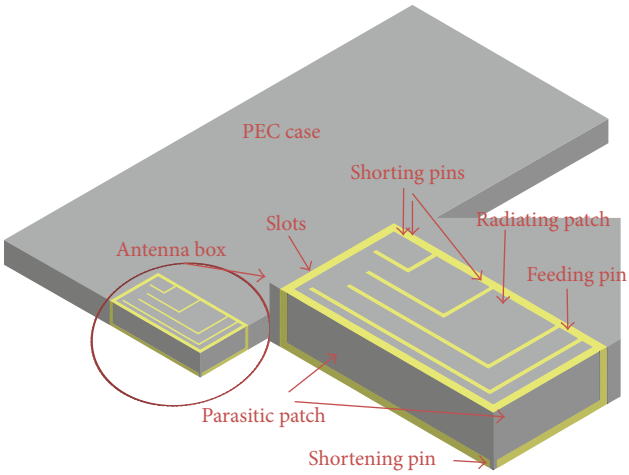

FIGURE 2: A 3D view of the model, parasitic patch, radiating patch, slots, and shortening pin.

2.2. Multiple Shorting Pins. In [16], a dual shorting pin PIFA model was proposed and designed for the dual band operations of mobile handsets. Multiple shorting pins provide different paths and lengths to the antenna for radiating multiple frequencies. Shorting pins provide multiple paths to currents and allow the antenna to radiate at multiple frequencies. In PIFA, the resonant frequency bands depend on both the position and width of the shorting pins used in the model [10]. Multiple shorting pins add stability to the antenna model by allowing it to maintain its performance in adverse situations. Shorting pins, when applied near the feed position, allow designers to reduce the size of the model. In our model, the positions of the shorting pins were chosen carefully to enhance the performance of the antenna at the desired frequency bands and to suppress undesired frequencies.

2.3. Parasitic Patch. A parasitic patch is used to control the directivity and is useful in many ways specially designing low profile antennas. The parasitic patch has a dual effect on S11, when used with the PEC and PMC boundaries. The two sides of the *antenna box* shown in Figure 3 are being used as a parasitic patch to improve the S11 result of our design. Parasitic patches are widely being used in antennas to change the radiating field patterns, steer the beam, and increase the bandwidth [12]. The parasitic patch in our model is used with PEC boundary. Parasitic patch with the PMC boundary may act like a high impedance surface (HIS) [17]. HIS based antennas are extensively being used in vehicular antennas.

2.4. Tempering the Substrate. Dielectric materials like FR-4 are used in antenna designs for many reasons. One aspect is that because it allows miniaturization of the antenna model, and at the same time it is very cheap. However, the problem with using a bulk of dielectric material in communication devices is that it effects the performance of the antenna in terms of efficiency. Because of antenna size limitations (as

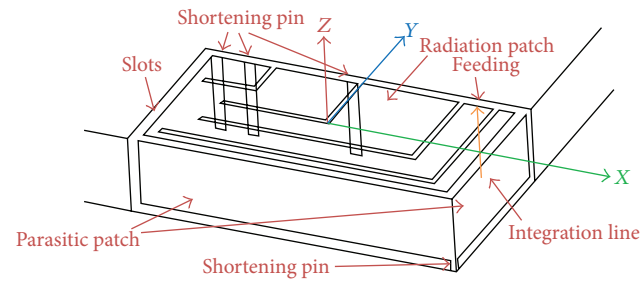

FIGURE 3: A 3D view of the antenna box, radiating patch, parasitic patch, feeding, and shorting pins.

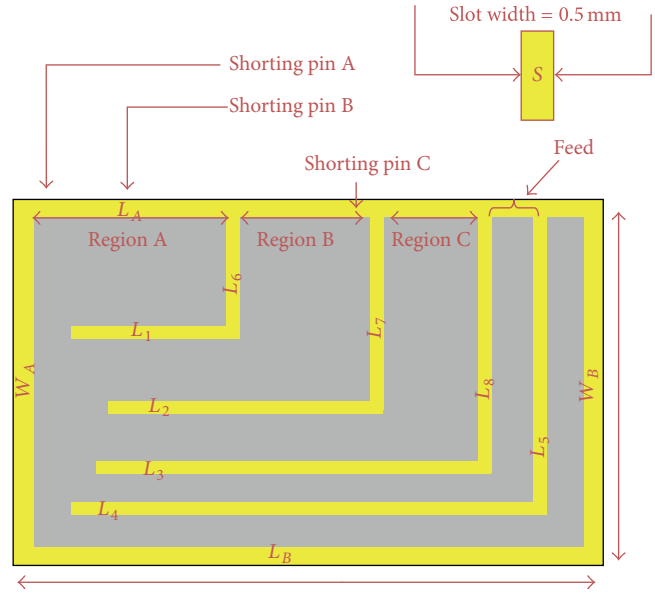

FIGURE 4: Parametric description of the slots in the radiation patch.

we cannot go on increasing the height of our model), it becomes an energy storing device which may be referred to as a lossy device. To deal with this situation, as shown in Figure 5, four vacuum gaps are inserted in the substrate at different positions and the width has been swept for multiple values to ultimately make the proposed model radiate the maximum energy with improved efficiency [18]. The purpose of an antenna is to radiate a signal that is fed to it and not to store it and increase the antenna losses. In [19], substrates are discussed, which can be used in antenna designs. Moreover, the effects of different substrates on the performance of antennas are also highlighted to control the antenna losses.

In our model, we have inserted vacuum gaps inside the FR-4 dielectric material (which we refer to as substrate tempering), for which both the position and width of the vacuum gap affect the S11 results of our model. Moreover, the results show that tempering the substrate material may also improve the gain in the resonant bands of the antenna [20–25].

Because the proposed antenna model is a kind of cavity, the cavity perturbation method can be applied to it. Any increment or decrement in ε or μ at any point in the cavity

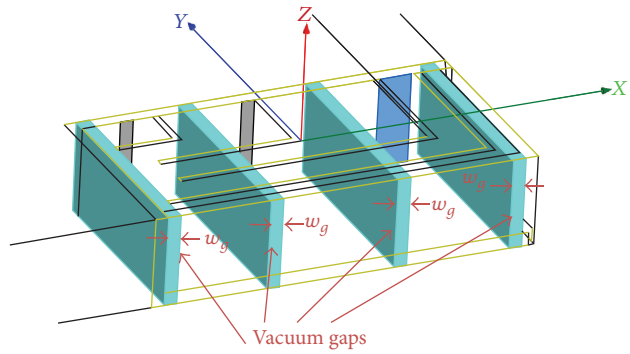

FIGURE 5: Substrate tempering by inserting vacuum gaps in FR-4.

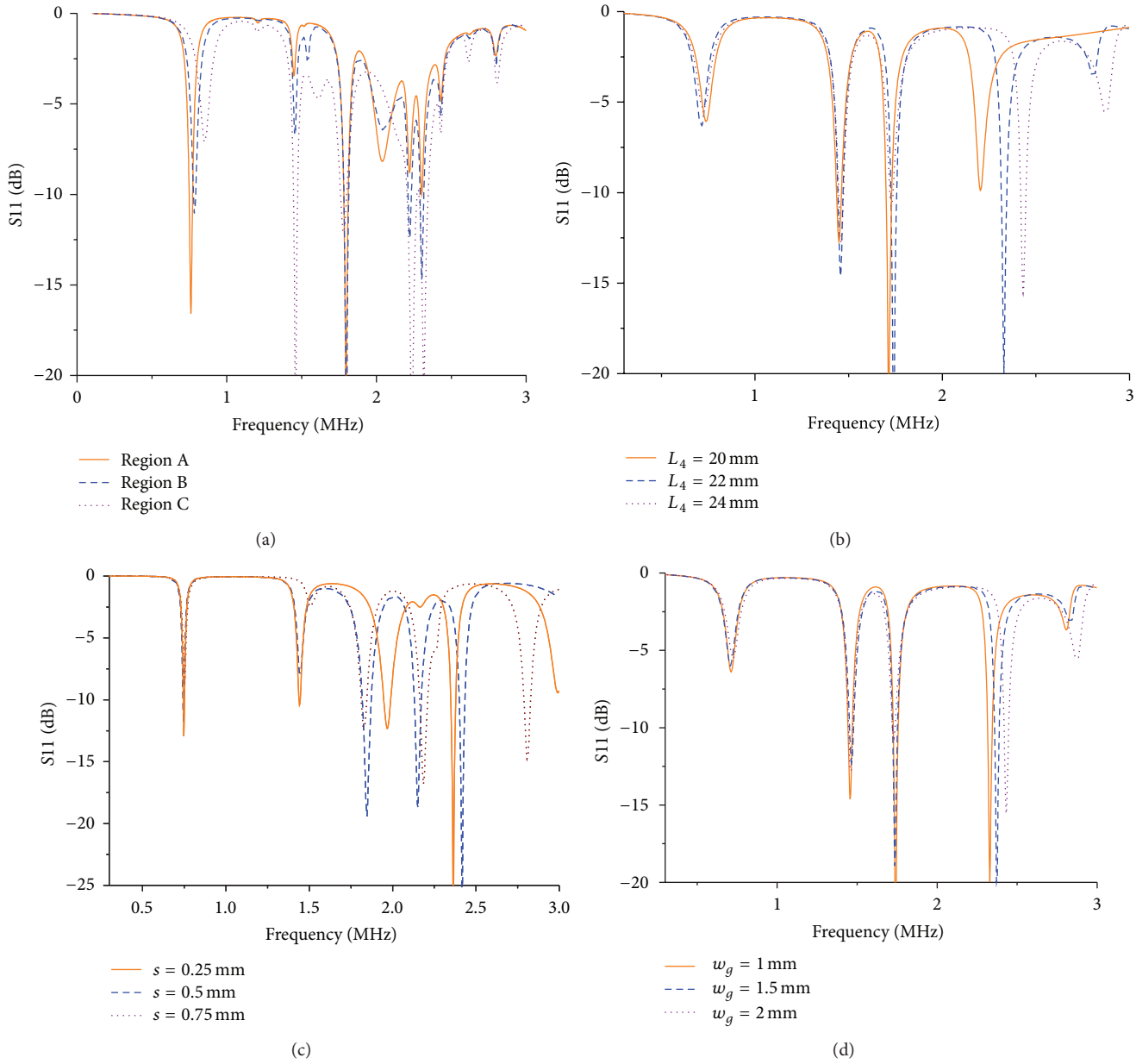

FIGURE 6: (a) Shorting pins position effect on S11. (b) Effect of slot length on S11. (c) Effect of slot width on S11. (d) Effect of varying the width of vacuum gaps inserted in FR-4 substrate on S11.

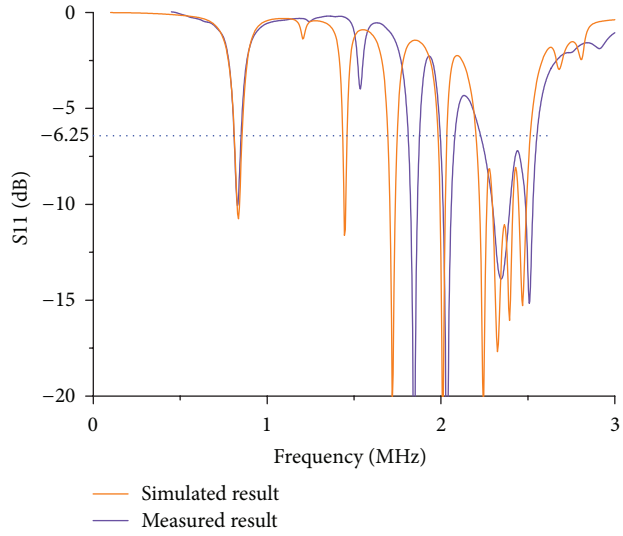

Figure 7: Comparison of simulated and measured S11 results for the proposed model.

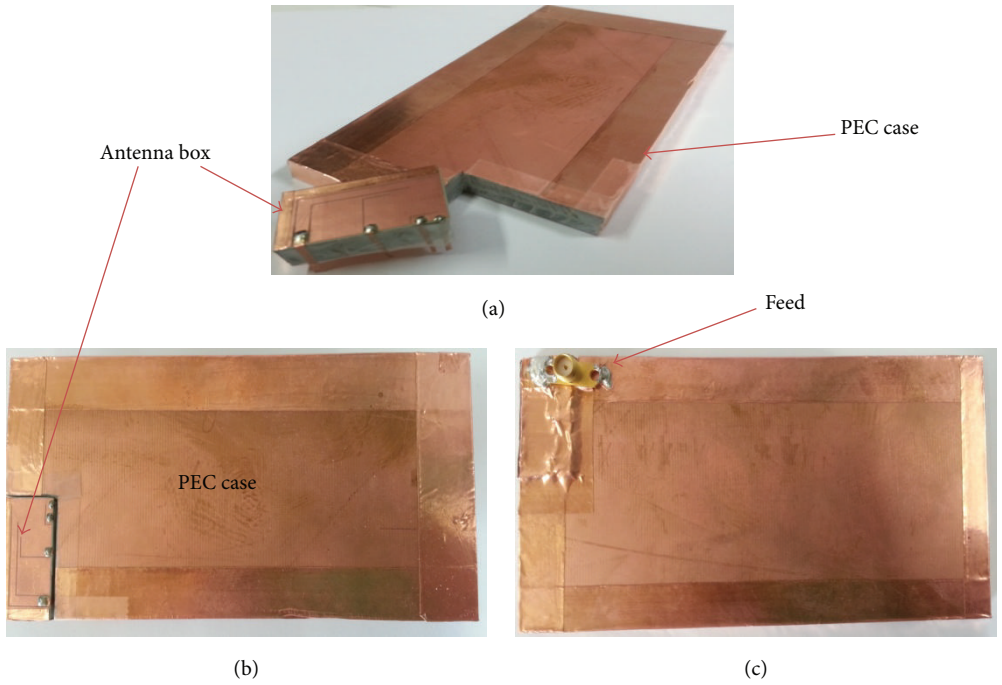

Figure 8: (a) Antenna box and *PEC case*. (b) Top view. (c) Bottom view.

may decrease or increase the resonant frequency of the cavity. Moreover, change in resonant frequency can also be related to the stored electric and magnetic energies inside the cavity as well. We choose the orientation and position for the vacuum gap using parametric sweep option in 3D simulation tool used for designing this model. Considering that the fields inside the cavity are approximately the same before and after the substrate tempering or perturbation, we may conclude that the resonant frequency of the cavity may increase or decrease after tempering the substrate depending upon the position of tempering or perturbation inside the cavity [26, 27].

3. Results and Discussion

The proposed model is simulated with the High Frequency Structural Simulator (HFSSv13.0) and a prototype for the proposed model is also designed. The comparison of the simulated and measured S11 results is shown in Figure 7. Section 3.1 deals with the benefits of the enhancements we applied to the model. In Section 3.2, S11 and the magnitude of the E-field at the corresponding resonant frequencies are elaborated. Section 3.3 covers the details of the bandwidths and the gains at corresponding resonant frequencies.

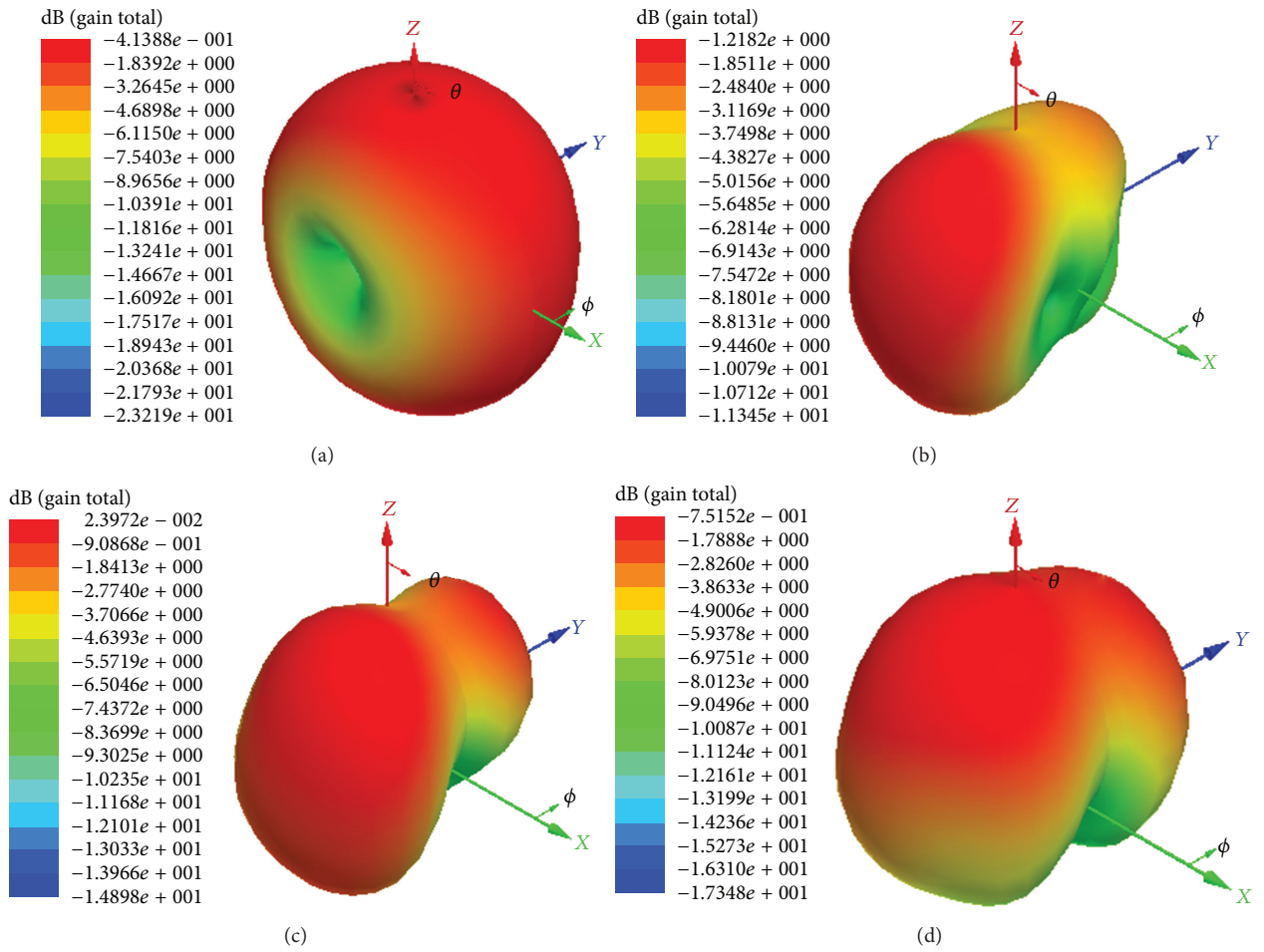

FIGURE 9: (a) Gain at the resonant frequency 875 MHz. (b) Gain at the resonant frequency 1.735 GHz. (c) Gain at the resonant frequency 2.035 GHz. (d) Gain at the resonant frequency 2.35 GHz.

3.1. Effects of the Enhancements. The enhancements that we have applied to the proposed model have resulted in allowing us to obtain the wide bandwidths at the resonant frequencies. The enhancements are inserting slots in the radiating patch, a parasitic patch with the PEC boundary, multiple shorting pins, and substrate tempering by inserting vacuum gaps inside the FR-4 substrate. The effects of these enhancements on the S11 curve are clear in Figure 6.

In Figure 6(a), the shift in the resonant frequency bands is shown when shorting pins are swept along region A, region B, and region C as mentioned in Figure 4. The S11 result in Figure 6(a) clearly shows that the PIFA model provides a narrow bandwidth when the shorting pins are close to the feeding pin. Because the electric length between region A and the feed point is the shortest compared to regions B and C, the bandwidth is narrow. When shorting pins are applied in region C, the bandwidth is wider. To increase the bandwidth of our proposed model, the shorting pins can be swept along regions A, B, and C, respectively.

In Figures 6(b) and 6(c), the effects of varying the slot length and slot width on the S11 curve are shown. Figure 6(b) shows the effect of changing the length of slot L_4 (shown in Figure 4). The simulated S11 results for three different values of the slot length are evident that changing the length of slot L_4 (L_4 = 20 mm, L_4 = 22 mm, and L_4 = 24 mm) effects the extreme resonant bands by and large. The effect on the lower resonant band is minor but the higher resonant band is almost shifted completely, which is favorable in cases where higher resonant bands need a shift. On the other hand, the middle resonant band has remained fixed. In Figure 6(c), the S11 results show that changing the slot width also affects the S11 curve. It is clear that another way to shift the resonant bands could be just by varying the slot width. The S11 results are presented for three different values of slot width, that is, s = 0.25 mm, s = 0.5 mm, and s = 0.75 mm. The resonant bands at higher frequencies shift their positions in the simulated S11 curve and the lowest band remains unchanged.

Furthermore, to improve the efficiency and gain another enhancement we used was to insert the vacuum gaps inside the dielectric material which we denote as substrate tempering. The width and position of the vacuum gaps affect the S11 curve which is shown in Figure 6(d). For three different values of vacuum gap widths, that is, w_g = 1 mm, w_g = 1.5 mm, and w_g = 2 mm, the S11 results show that

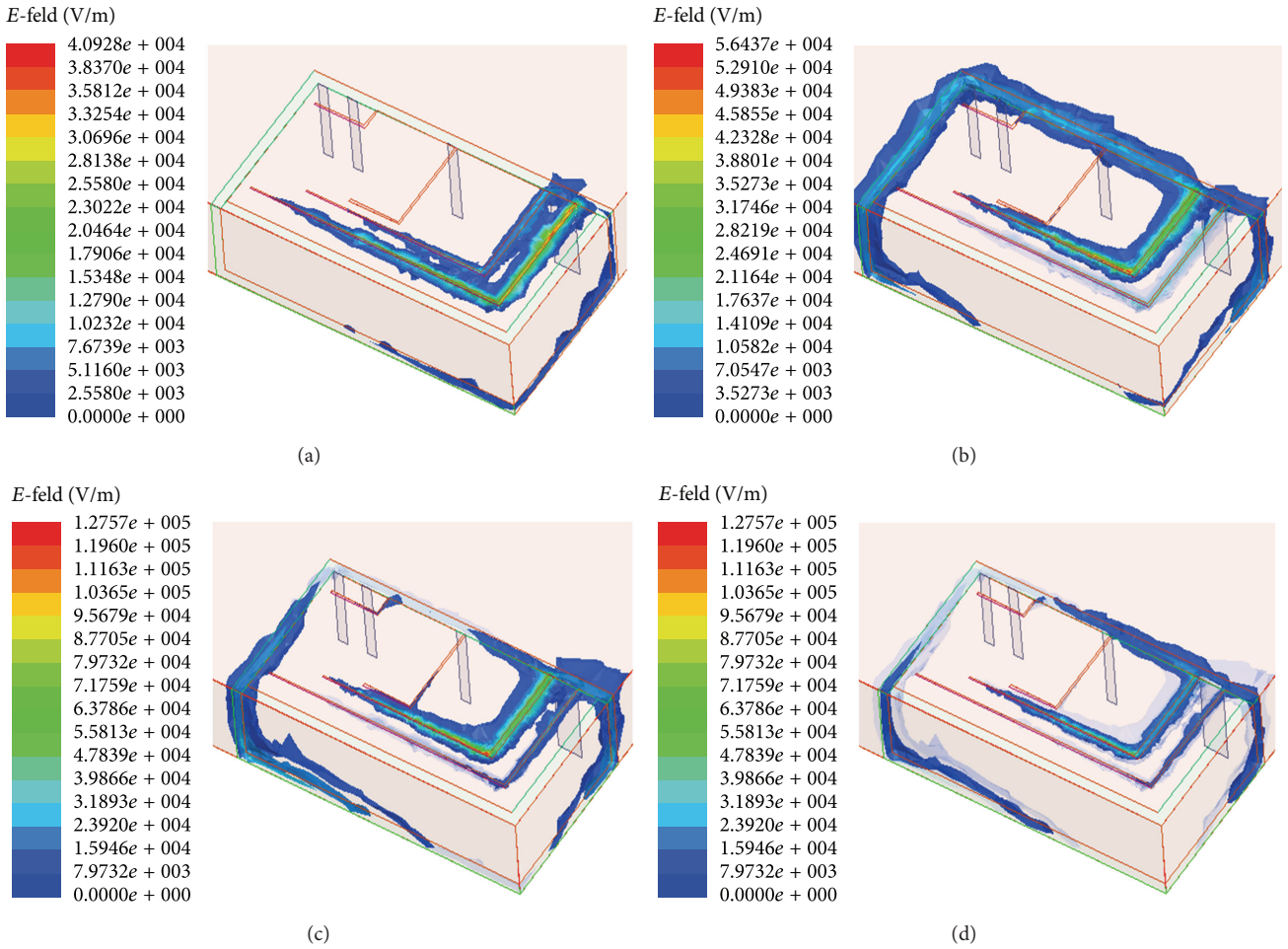

Figure 10: (a) Magnitude of the E-field at resonant frequency 875 MHz. (b) Magnitude of the E-field at resonant frequency 1.735 GHz. (c) Magnitude of the E-field at resonant frequency 2.035 GHz. (d) Magnitude of the E-field at resonant frequency 2.35 GHz.

changing the width of the vacuum gaps affect the higher resonant band of frequencies because it shifts them further towards the higher frequency regions which is in agreement with our previous discussion that dielectric materials help to miniaturize antenna models. Tempering the substrate can help in two ways; one way is to shift the resonant band and the other way is to increase the efficiency of the antenna design. In our proposed model, tempering helped in both ways. Shifting of the higher resonant band with substrate tempering is realized in Figure 6(d). In Section 3.2 along with the multiband resonant S11 curve, the magnitude of the E-field at corresponding resonant frequencies and improvement in gain due to substrate tempering are presented and discussed.

3.2. Characteristics of the Proposed Model. The properties of our proposed PIFA in terms of the S11 curve, the magnitude of the E-field at corresponding resonant frequencies, and the gain at the center of each resonant frequency bands are presented in this section. The optimized S11 result for the proposed model simulated with the HFSSv13.0 is shown in Figure 7, which has multiple resonant bands. The simulated S11 result is compared with the measured S11 and is close to agreement with each other. All the resonant bands are shifted a little towards right. It might be because of the fabrication tolerance. The resonant frequency bands mentioned in Figure 7 (1st, 2nd, 3rd, and 4th) are used in most communication devices for GSM, UMTS, Bluetooth, and WLAN. The gain for the corresponding resonant frequencies is shown in Figure 9, and it is in agreement with the requirements.

The gain for the corresponding resonant frequencies is shown in Figure 9 and meets the requirements. The gains at resonant frequencies are greater than the minimum value required by the communication devices that work on these frequency ranges. At 875 MHz in Figure 9(a), the gain is approximately −0.414 dB and its shape is just like a dipole field. Dipole like shape of the radiating field at lower resonant frequency is because *PEC case* and radiating patch both act like a dipole connected to the feed. For all the other resonant bands the field is being radiated in all the directions. Therefore, radiation pattern is like a monopole because radiating patch radiates field. The radiation pattern at higher resonant frequencies is roughly omnidirectional. At 1.735 GHz in Figure 9(b), the gain is −1.22 dB, and its shape is amorphous, but the directivity is such that it

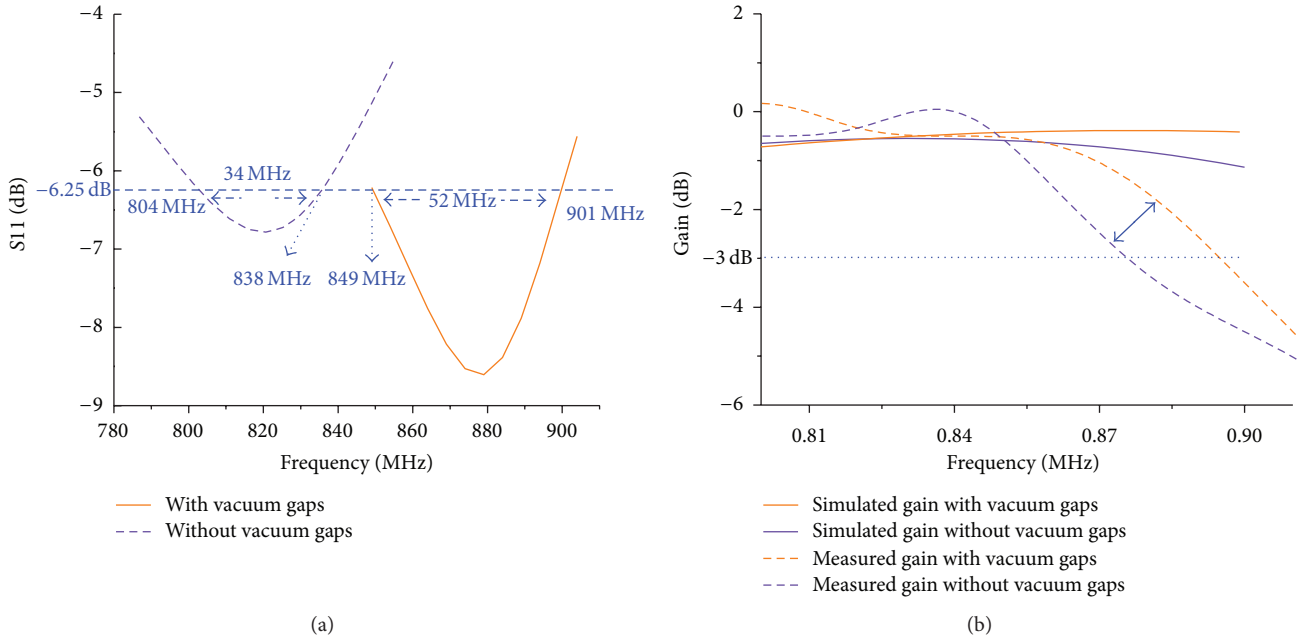

Figure 11: (a) Bandwidth comparison for the simulated substrate tempering at a resonant frequency band centered at 875 MHz. (b) Gain comparison with and without substrate tempering for the resonant frequency band centered at 875 MHz.

can offer a minimum SAR. In Figures 9(c) and 9(d), the gain at 2.035 GHz and 2.35 GHz is 0.024 dB and −0.75 dB, respectively. The directivity of the proposed model at higher frequencies has a roughly omnidirectional shape which is essential for many handheld communication devices working in this frequency range.

In Figure 10, the magnitude of the E-field at the corresponding resonant frequencies is shown. From these figures, we can determine the path followed by the current for every resonant frequency band. Different paths followed by the current on the radiating sheet are evident of the fact that inserting slots in the radiating patch provides multiple paths for the current to flow and therefore gives rise to multiple resonant frequencies. Furthermore, these resonant frequencies and corresponding bandwidths can be enhanced with shorting pins, parasitic patch, and other techniques.

3.3. Bandwidths and Corresponding Gains. In this section, the bandwidths, resonant frequencies, and gain for those corresponding bands of frequencies (1st, 2nd, 3rd, and 4th resonant bands) are discussed. The results show a wide bandwidth at the resonant frequencies. These are the optimized results of all the enhancements that we have applied to the proposed model which are discussed in Section 2 in detail.

In Figures 11(a) and 11(b), a comparison of the bandwidths and corresponding gains is presented. The optimized result for the proposed model at the 1st resonant band (lowest resonant band) shows a difference in the bandwidth and gain with and without tempering of the substrate. It is clear that inserting the vacuum gaps in the substrate, in order to exploit the impedance bandwidth Q, not only provides a wide bandwidth but also helps to improve the gain. In our proposed model, the simulated results show an increment in the bandwidth from 34 MHz to 52 MHz and gain is increased and stabilized. One should choose the position and width for the vacuum gap wisely (as already mentioned in Section 2.4, position is important because it defines whether the resonant frequency of the cavity is increased or decreased).

The gain is nearly flat and stable for all these resonant band of frequencies shown in Figure 12 and is preferred by most communications devices that work in this range of frequencies.

4. Conclusion

In this paper, a new design for a low profile PIFA model is presented. In general, applications may include communication devices that work for GSM 850/900, UMTS 850/900/1700/1900/2100, LTE 2300/2500, and ISM 2400 bands used for Bluetooth and WLAN. The design is unique and simple. In contrast to a traditional PIFA model, this design is covered with PEC boundaries from all sides. By introducing a few slots in the radiating patch, applying a parasitic patch, tempering the substrate, and using multiple shorting pins in the model, four resonant bands centered at 875 MHz, 1735 MHz, 2035 MHz, and 2350 MHz have been achieved with bandwidths of 52 MHz, 60 MHz, 73 MHz, and 319 MHz, respectively. The gain for the corresponding resonant bands is relatively flat. Multiple aspects of this design were studied which we have presented in this paper, and it is evident that this model has the ability to maintain its performance even in adverse and unfriendly environments. The proposed design methodology can be useful in low profile multiband resonant communication devices, in particular, in the design of antennas for mobile handsets.

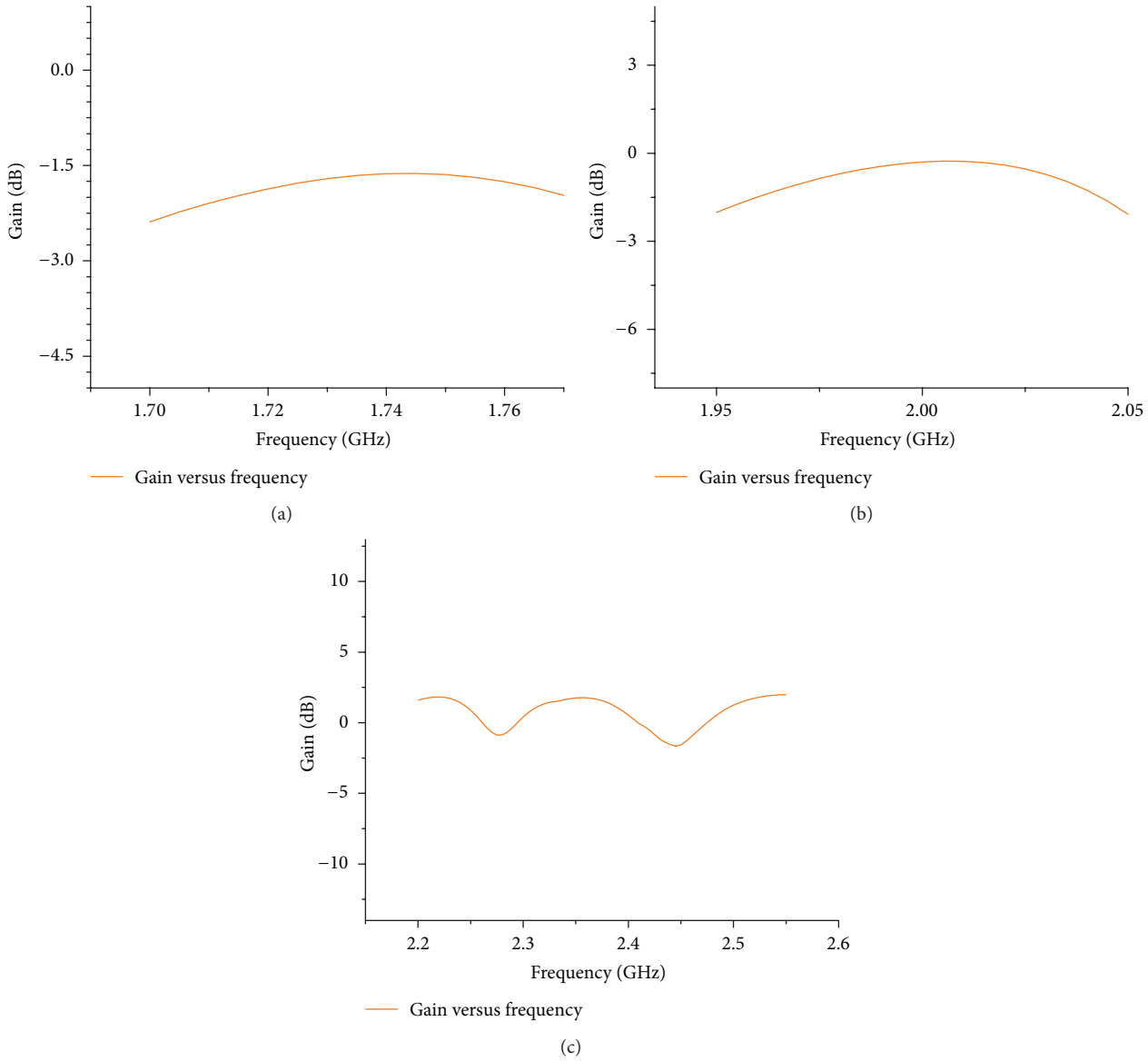

Figure 12: (a) Gain offered by the resonant band centered at 1.735 GHz. (b) Gain offered by the resonant band centered at 2.035 GHz. (c) Gain for the corresponding resonant band centered at 2.35 GHz.

Conflict of Interests

The authors declare that there is no conflict of interests regarding the publication of this paper.

Acknowledgment

This research was supported by the Research Fund BK21 plus of Kyungpook National University in 2013.

References

[1] H. T. Chattha, Y. Huang, and Y. Lu, "PIFA bandwidth enhancement by changing the widths of feed and shorting plates," *IEEE Antennas and Wireless Propagation Letters*, vol. 8, pp. 637–640, 2009.

[2] C. W. Chiu and F. L. Lin, "Compact dual-band PIFA with multi-resonators," *Electronics Letters*, vol. 38, no. 12, pp. 538–540, 2002.

[3] C. See, H. Hraga, and R. A. Hameed, "A low-profile ultra-wideband modified planar inverted-F antenna," *IEEE Transactions on Antennas and Propagation*, vol. 61, no. 1, pp. 100–108, 2012.

[4] N. Haider, D. Caratelli, and A. G. Yarovoy, "Recent developments in reconfigurable and multiband antenna technology," *International Journal of Antennas and Propagation*, vol. 2013, Article ID 869170, 14 pages, 2013.

[5] A. Cabedo, J. Anguera, C. Picher, M. Ribó, and C. Puente, "Multiband handset antenna combining a PIFA, slots, and

ground plane modes," *IEEE Transactions on Antennas and Propagation*, vol. 57, no. 9, pp. 2526–2533, 2009.

[6] J. S. McLean, "A re-examination of the fundamental limits on the radiation Q of electrically small antennas," *IEEE Transactions on Antennas and Propagation*, vol. 44, no. 5, pp. 672–676, 1996.

[7] D. F. Sievenpiper, D. C. Dawson, M. M. Jacob et al., "Experimental validation of performance limits and design guidelines for small antennas," *IEEE Transactions on Antennas and Propagation*, vol. 60, no. 1, pp. 8–19, 2012.

[8] M. Koubeissi, M. Mouhamadou, C. Decroze, D. Carsenat, and T. Monédière, "Triband compact antenna for multistandard terminals and user's hand effect," *International Journal of Antennas and Propagation*, vol. 2009, Article ID 491262, 7 pages, 2009.

[9] T. Tashi, M. S. Hasan, and H. Yu, "Design and simulation of UHF RFID tag antennas and performance evaluation in presence of a metallic surface," in *Proceedings of the 5th International Conference on Software, Knowledge Information, Industrial Management and Applications (SKIMA '11)*, vol. 1, pp. 1–5, Benevento, Italy, September 2011.

[10] D. Qi, B. Li, and H. Liu, "Compact triple-band planar inverted-F antenna for mobile handsets," *Microwave and Optical Technology Letters*, vol. 41, no. 6, pp. 483–486, 2004.

[11] M. S. Kim, "PIFA device for providing optimized frequency characteristics in a multi-frequency environment and method for controlling the same," US patent application US 7 385 557 B2, 2008.

[12] W. K. W. Ali, "Broadband square microstrip patch antenna with suspended parasitic element," in *Proceedings of the 6th International Symposium on Antennas, Propagation and EM Theory*, pp. 50–53, Beijing, China, November 2003.

[13] A. Moleiro, J. Rosa, R. Nunes, and C. Peixeiro, "Dual band microstrip patch antenna element with parasitic for GSM," in *IEEE Antennas and Propagation Society International Symposium*, vol. 4, pp. 2188–2191, Salt Lake City, Utah, USA, July 2000.

[14] Y. Belhadef and N. B. Hacene, "Design of new multiband slotted PIFA antennas," *International Journal of Computer Science Issues*, vol. 8, no. 4, pp. 325–330, 2011.

[15] W. F. Richards, S. Davidson, and S. A. Long, "Dual-band reactively loaded microstrip antenna," *IEEE Transactions on Antennas and Propagation*, vol. 33, no. 5, pp. 556–561, 1985.

[16] H. Wong, K. M. Luk, and C. H. Chan, "Small antennas in wireless communications," *Proceedings of the IEEE*, vol. 100, no. 7, pp. 2109–2121, 2012.

[17] M. Sonkki, M. Cabedo-Fabrés, E. Antonino-Daviu, M. Ferrando-Bataller, and E. T. Salonen, "Creation of a magnetic boundary condition in a radiating ground plane to excite antenna modes," *IEEE Transactions on Antennas and Propagation*, vol. 59, no. 10, pp. 3579–3587, 2011.

[18] A. D. Yaghjian and S. R. Best, "Impedance, bandwidth, and Q of antennas," *IEEE Transactions on Antennas and Propagation*, vol. 53, no. 4, pp. 1298–1324, 2005.

[19] A. O. Karilainen, P. M. T. Ikonen, C. R. Simovski et al., "Experimental studies on antenna miniaturisation using magneto-dielectric and dielectric materials," *IET Microwaves, Antennas & Propagation*, vol. 5, no. 4, pp. 495–502, 2011.

[20] Y.-T. Jean-Charles, V. Ungvichian, and J. A. Barbosa, "Effects of substrate permittivity on planar inverted-F antenna performances," *Journal of Computers*, vol. 4, no. 7, pp. 610–614, 2009.

[21] G. A. E. Vandenbosch, "Reactive energies, impedance, and Q factor of radiating structures," *IEEE Transactions on Antennas*, vol. 58, no. 4, pp. 1112–1127, 2010.

[22] S. A. Long, "A mathematical model for the impedance of the cavity-backed slot antenna," *IEEE Transactions on Antennas and Propagation*, vol. 25, no. 6, pp. 829–833, 1977.

[23] H. K. Smith and P. E. Mayes, "Stacking resonator to increase the bandwidth of low profile antennas," *IEEE Transactions on Antennas and Propagation*, vol. 35, no. 12, pp. 1473–1476, 1987.

[24] J. Eichler, P. Hazdra, M. Capek, and M. Mazanek, "Modal resonant frequencies and radiation quality factors of microstrip antennas," *International Journal of Antennas and Propagation*, vol. 2012, Article ID 490327, 9 pages, 2012.

[25] M. Capek, P. Hazdra, and J. Eichler, "A method for the evaluation of radiation Q based on modal approach," *IEEE Transactions on Antennas and Propagations*, vol. 60, no. 10, pp. 4556–4567, 2012.

[26] P. Vainikainen, J. Ollikainen, O. Kivekäs, and I. Kelander, "Resonator-based analysis of the combination of mobile handset antenna and chassis," *IEEE Transactions on Antennas and Propagation*, vol. 50, no. 10, pp. 1433–1444, 2002.

[27] D. M. Pozar, *Microwave Engineering*, John Wiley & Sons, New York, NY, USA, 2nd edition, 1998.